



Design, optimization and experimental verification of UWB-MIMO antenna with WLAN and complete X-band notched characteristics, checked with characteristic mode analysis (CMA)

B. Rama Rao¹ · K. S. Chakradhar² · D. Nataraj³

Received: 9 January 2022 / Revised: 10 June 2022 / Accepted: 6 February 2023 / Published online: 20 February 2023
© The Author(s), under exclusive licence to Springer Science+Business Media, LLC, part of Springer Nature 2023

Abstract

In this proposed work, a compact Multiple Input Multiple Output (MIMO) antenna is designed for Ultra-Wide Band applications with dual-notch band characteristics is presented. Widely available low cost FR4 substrate is used for fabrication and the overall dimensions of the antenna are $24 \times 36 \text{ mm}^2$ ($0.248 \lambda_0 \times 0.372 \lambda_0$, λ_0 measured at lower band) having a height of 1.6 mm, dielectric constant 4.4. The proposed dual-band MIMO antenna operates from 3.1 to 13.4 GHz and an isolation higher than 15 dB is achieved in the entire working band with notched bands at Wireless Local Area Network (WLAN) and X-bands. The obtained radiation efficiency values are above 90% with a maximum value of 97% at 4 and 7 GHz bands and higher peak gain values are achieved with a maximum value of 7.4 dBi at the operating bands. The MIMO checking parameters (Envelope Correlation Coefficient, Diversity Gain, Total Active Reflection Coefficient, Channel Capacity Losses and Mean Effective Gain) are also presented for the proposed design giving good diversity performance characteristics in the entire operating band and also at the notch bands. The 3D polar plots are presented for the proposed design is providing high gain values and also presented negative gain is occurred at notched bands. The proposed single notched design S-parameters results are checked with Characteristic Mode Analysis. The fabricated model is tested and verified experimentally and these values are well matched with simulated once.

Keywords MIMO · UWB · Isolation · Band notched · WLAN · CMA · Complete X-band

1 Introduction

The present wireless communication technology is upgrading rapidly day by day, because of the developments in miniaturized and portable wireless devices, reduction of time allocation and high speed transmission. The high

speed communication mainly depends on applied transmitted power and bandwidth. The transmitted power can't be increased, as it effects the battery performance of the device and hence, the alternative is to increase the bandwidth. A large bandwidth 7.5 GHz (3.1–10.6 GHz) is assigned as unlicensed for commercial applications in 2002 by Federal Communication Commissions (FCC) and it is named as Ultra-Wide Band (UWB) technology [1]. The several inherent applications of UWB technology are imaging (brain tumor and cancer cells detections) applications, vehicular RADAR applications and Wireless Body Area Network (on body and off body) applications [2]. In short distance communication like indoor applications, a serious problem called as multipath fading occurs. Recently, a new wireless communication technology emerged to avoid the fading problems by increasing the number of terminals at transmitting as well as receiving side and is termed as Multiple Input Multiple Output (MIMO) technology. The combined form of UWB and MIMO gives high speed transmission without any fading problems in wireless communications. But, due

✉ K. S. Chakradhar
kdrchakradhar@gmail.com

B. Rama Rao
drbrrao2015@gmail.com

D. Nataraj
dasari.nataraj@gmail.com

¹ ECE Department, Aditya Institute of Technology and Management, Tekkali, A.P., India

² ECE Department, Sree Vidyanikethan Engineering College, Tirupathi, A.P., India

³ ECE Department, Pragati Engineering College, Kakinada, A.P., India

to the smaller spacing between elements in portable devices, coupling comes into picture [3, 4]. The several UWB-MIMO antennas with different decoupling structures are presented in the literature [5–10]. Several designs like Fence-type structure [5], Electromagnetic Band Gap structure [6], metamaterial structures [7], digitated Parasitic structure [8], simple stubs between radiators [9] and diagonally placed stub with Defected Ground Structure (DGS) [10] are available in the current literature. All the above works [5–10] are working in the range of UWB band for short distance communications.

Some times the UWB signal is effected with other signals like World wide Interoperabilty Microwave Access [WiMAX (3.3–3.7 GHz)], Wireless Local Area Network [WLAN (5.15–5.85)] and X-band satellite up (7.9–8.4 GHz) & down link (7.25–7.75 GHz) frequency bands. Hence, to avoid the collision between UWB and the above mentioned bands, different band-notch techniques are proposed by authors as listed [11–19]. WLAN band (5.15–5.92 GHz) is rejected by making bent slit on radiator [11], WLAN band included in the band of 3.96–6.2 GHz is prevented by interdigital capacitance concept [12], WLAN band (4.8–6.2 GHz) can be rejected by PIN diodes [13], 4.4–6.2 GHz band is filtered by making slot on rectangular ring radiator [14], WLAN band rejection is done by making folded slots on radiators [15], by removing the L-shaped slits on ground plane, the WLAN band is filtered from UWB band [16], WLAN band is removed by making inverted C-slot on top layer [17], curved U-shaped slot on radiator [18], stright U-shaped slot on top layer [19].

The above mentioned works [11–19] are proposed to mostly reject the WLAN band. But, in some cases UWB signal is facing collision problems with X-band up & down link frequencies along WLAN band. The authors in the literature has done good work on rejection of X-band along with WLAN are listed [20–25]. The lower WLAN (around 5.6 GHz) band and X-band (around 8 GHz) satellite up link frequencies are rejected by making inverted U and L shaped slot on ground plane [20], an inverted C-slot on radiator and an arc shaped strip protruded to the ground plane are used for the rejection of X-band down link frequency and WLAN band respectively as mentioned in [21], two inverted L-shaped slots and hook shaped slots on radiator are used for the removing the WLAN and INSAT-C bands [22, 23], an upward and downward direction C-slots are etched on radiator for filtering the WLAN and WiMAX bands respectively [24], WLAN and X band (up link) frequencies are rejected by protruding open and closed rectangular strips to the ground plane [25], C-slot on radiator and an inverted L stub are protruded to the ground to reject the WLAN and X-band up link frequencies in the UWB region [26]. In the above literature, various research works for the rejection of WLAN and X-band (either up or down link frequencies but not completely X-band which is from 8 to

12 GHz) are presented. But the proposed work is designed for UWB band (3.1–13.4 GHz) applications with dual-band notched characteristics. The notched bands include WLAN (5.15–5.85 GHz) and complete X-band (8–12 GHz).

The advantages of proposed work compared with other listed literature works: (1) The antenna size is compact of size $24 \times 36 \text{ mm}^2$, i.e. low profile, easy to design and simple decoupling structure; (2) Complete band rejections of WLAN and X-band are achieved with simple slots on the top plane; (3) Stable radiation patterns with bore sight gain are achieved in the working UWB region and also a high gain of 7.14 dBi are achieved in the X-band region; (4) Checked the S-parameter results with CMA and (5) Showing the negative gain in notched bands using 3D polar plots and also checked the same with peak gain response.

The proposed MIMO work is designed for UWB applications with complete band rejections of WLAN and X-bands. An isolation more than 22 dB is achieved with simple parasitic strip placed between the radiators except at mid band frequencies. The overall size of the structure is $24 \times 36 \times 1.6 \text{ mm}^3$ and working band of the structure is 3.1–13.4 GHz with band notched frequencies at 5.15–5.85 GHz & 8–12 GHz. The peak gain values vary from 2.5 to 7.4 dBi in the working band and efficiency values are 90% except at notched band regions. The diversity metrics ECC, DG, TARC, CCL and MEG are checked with measured results and all are well matched. Section 2 discuss the antenna design, evolution and optimisation of the parameters. The complete discussions on results which includes S-parameters, diversity performance and radiation performance are represented in Sect. 3. Finally, Sect. 4 describes the conclusions.

2 Antenna design process and optimization of parameters

2.1 Antenna design and evolution

The proposed design comprises of two radiating patches with modified circular slots and T-shaped parasitic strip protruded on defected ground structure. It is designed and developed on a low cost FR4 dielectric substrate with constant 4.4, loss tangent 0.02. The structure is designed using Ansoft High Frequency Structure Simulator (HFSS) version 19 (Electronic Desk Top-18) and the overall structure size is $24 \times 36 \times 1.6 \text{ mm}^3$. The structure operates in the band of 3.1–13.4 GHz with an isolation of above 22 dB in majority of the band. The Fig. 1(a)–(c) represent the top and bottom views along with dimensional parameters and also with slot dimensional parameters. The dimensional parameter values are represented in Fig. 1(d) and 3D view of proposed design is represented in Fig. 1(e). The simulated S-parameters of Fig. 1(a) is represented is depicted in Fig. 2 and it observed

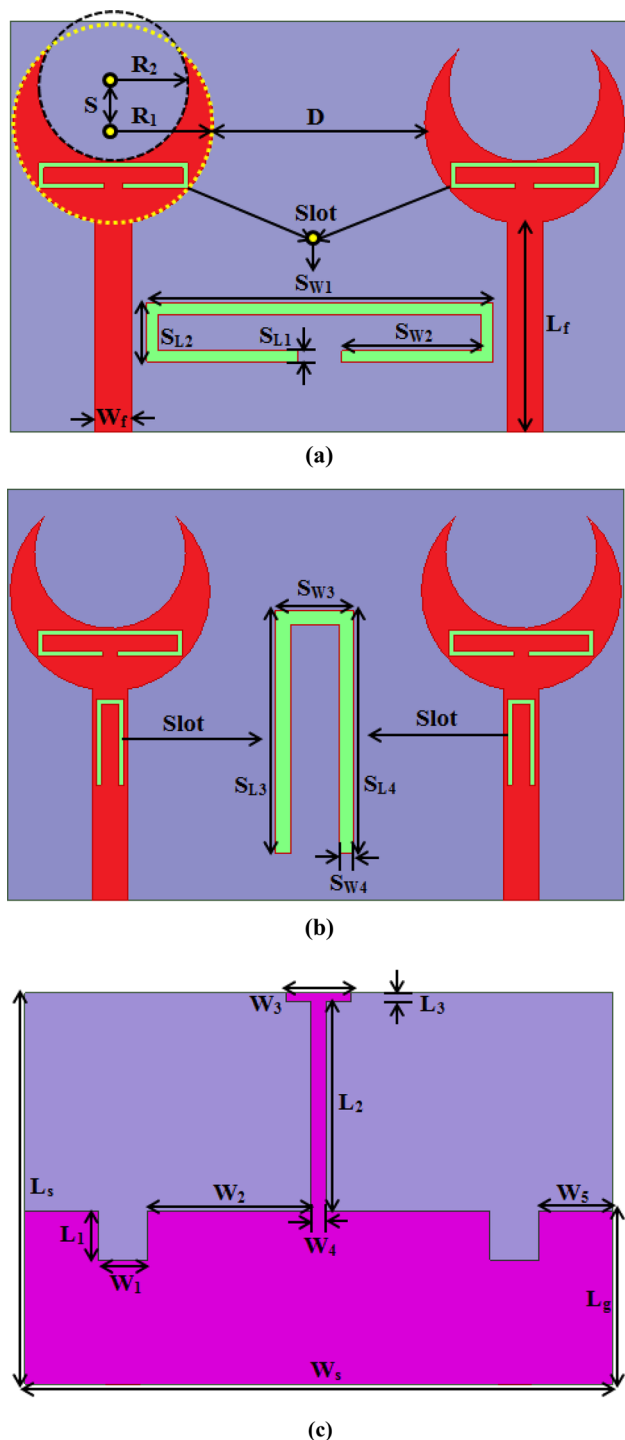


Fig. 1 Dimensional parameters of proposed antenna; **a** top layer (single notch); **b** top layer (dual notch); **c** bottom layer; **d** proposed antenna parameter with values and **e** 3D view of proposed antenna

that it is working in 3–13.2 GHz band with complete band rejection of WLAN (5.15–5.85 GHz) band.

2.1.1 Proposed single antenna evolution

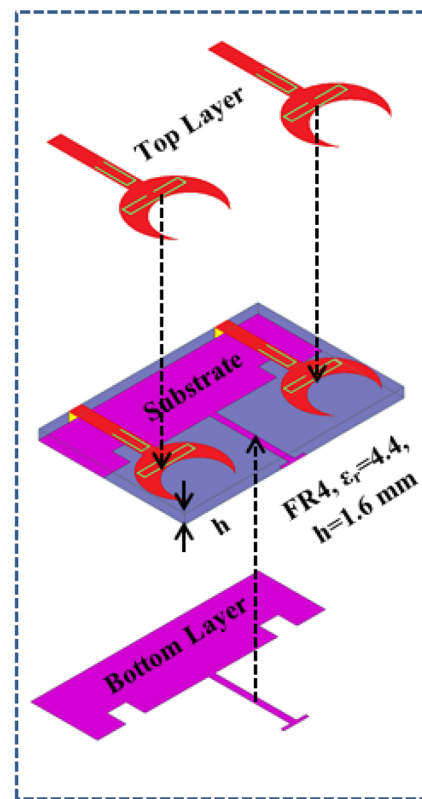
Initially the work begins with simple circular patch radiator of radius 5.8 mm with partial ground plane, and is named as single antenna @1. It is operating between 4.4 and 12.3 GHz except mid band which is from 5.8 to 7.2 GHz. The single antenna @2 is formed by extending the ground by protruding an inverted L-strip to the partial ground plane and also small circle of radius 4.4 mm is subtracted from circular patch. The inverted L-strip acts as reflector and, which shifts the lower band frequency 4.4–3.4 GHz i.e., nearly 1 GHz frequency shifting is obtained with reflector and is clearly shown in Fig. 8. Finally, a downward direction C-slot is itched on the radiator to get notching at WLAN band, and then single antenna @3 is formed. The final antenna operates from 3.4 to 13 GHz except at notched band, which is from 4.9 to 6.1 GHz. The evolution steps and corresponding S-parameters are clearly shown in Figs. 3 & 4. But the proposed single antenna does not cover the lower band of UWB region, and hence two element analysis is processed in the next part of the work.0

2.1.2 Proposed single notched MIMO antenna evolution

2.1.2.1 Evolution and analysis The evolution of proposed single notched MIMO antenna is represented in five steps. Initially, in step@1 two circular patches with partial connected ground is designed on 24×36 mm² sized FR4 substrate with dielectric constant 4.4 and operating from 4.4 to 12 GHz. In step @2 a small circle of radius 4.4 mm is placed on top side of the patch and it is subtracted from radiator. Due to the subtraction, the impedance matching is obtained at mid band frequency compared to the step @1. In step @3, two 3 mm×3 mm sized square patches are subtracted from the ground plane at the centre of feed line. In this stage, the structure operates in the 4.4–10.6 GHz band without impedance mismatches in the mid band range. However, entire UWB region is not covered as well as higher coupling is introduced between the radiators. To enhance the isolation, an optimised T-strip is placed between them, resulting in the enhanced isolation of 20 dB and at the same time obtaining impedance matching using the stub. The resulting antenna operates in the region 3–13.1 GHz covering the entire UWB region and X-band region. In step @5, to avoid the interference with WLAN band an optimised downward direction C-slot is introduced on the radiator. Due to slot etching on the radiator, the frequency band in the range 5.1–6 GHz is rejected. The evolution steps of proposed single notched MIMO antenna and corresponding S-parameters are represented in Figs. 5, 6 and 7. Finally the proposed structure operates from 3 to 13.2 GHz obtaining dual-notched band and an isolation of above 22 dB is achieved in the majority of the band.

$L_s = 24 \text{ mm}$, $W_s = 36 \text{ mm}$, $R_1 = 5.8 \text{ mm}$,
 $R_2 = 4.4 \text{ mm}$, $S = 2.4 \text{ mm}$, $D = 12.5 \text{ mm}$,
 $W_f = 2.1 \text{ mm}$, $L_f = 12.2 \text{ mm}$, $S_{w1} = 8.7 \text{ mm}$,
 $S_{w2} = 3.8 \text{ mm}$, $S_{L1} = 0.3 \text{ mm}$, $S_{L2} = 1.2 \text{ mm}$,
 $S_{w3} = 1.6 \text{ mm}$, $S_{w4} = 0.3 \text{ mm}$, $S_{L3} = 4.0 \text{ mm}$,
 $S_{L4} = 4.0 \text{ mm}$, $L_g = 10.6 \text{ mm}$, $L_1 = 3.0 \text{ mm}$,
 $L_2 = 12.9 \text{ mm}$, $L_3 = 0.5 \text{ mm}$, $W_1 = 3.0 \text{ mm}$,
 $W_2 = 10.0 \text{ mm}$, $W_3 = 4.0 \text{ mm}$, $W_4 = 1.0 \text{ mm}$,
 $W_5 = 4.5 \text{ mm}$.

(d)



(e)

Fig. 1 (continued)

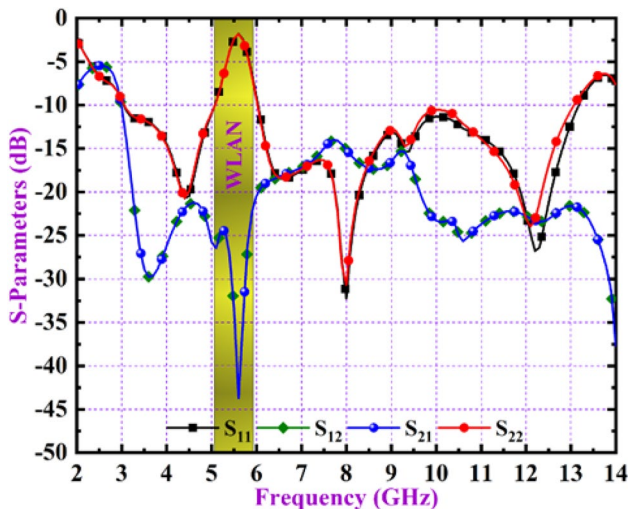


Fig. 2 Simulated S-parameters of proposed single notched MIMO antenna characteristics

The surface current distributions of proposed single notched MIMO antenna at various evolution stages are represented in Fig. 12. From Fig. 8, it is clearly observed

that the surface currents are obstructed to flow from one radiator to the other using the strip.

2.1.2.2 Parameters optimisation For getting the required bandwidth and desired stop band frequencies, parametric analysis has been done on dimensional parameters of proposed single notched antenna. The parameters are width of the feed (W_f), subtracted patch radius (R_2), length of ground (L_g), width of T-strip at top position (W_3), width of T-strip at bottom position (W_4) and width of downward direction C-slot (S_{w2}). The impact of these parameters on the impedance bandwidth performance of the antenna is represented in Table 1. From the Table 3, it is clearly observed that all the optimised parameters are observed to effect the impedance matching of the antenna. In the case of parameter optimisation of width of T-strip shows that for all values the impedance matching seems to be same. But, when $W_3 = 2 \text{ mm}$ & 6 mm the reflection coefficient values are closer to the -10 dB line. Hence, $W_3 = 4 \text{ mm}$ is chosen as optimised dimensional value. The Fig. 9 depicts the parameters optimisation of proposed single notched MIMO antenna.

2.1.2.3 Surface current distribution (SCD) The surface current distribution (SCD) is one of the important visual

Fig. 3 Evolution steps of proposed single antenna

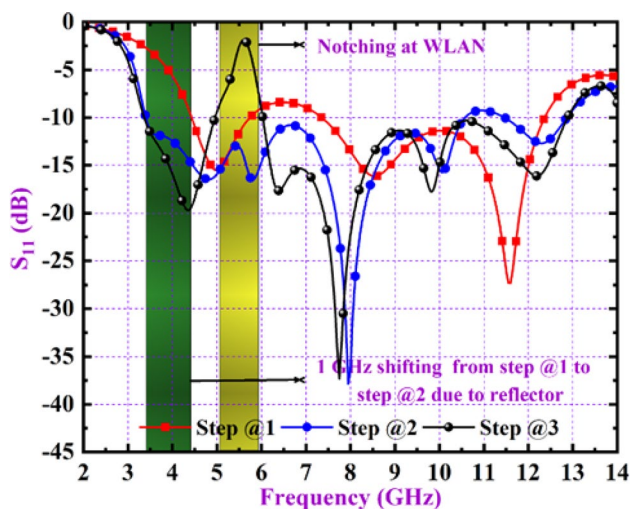
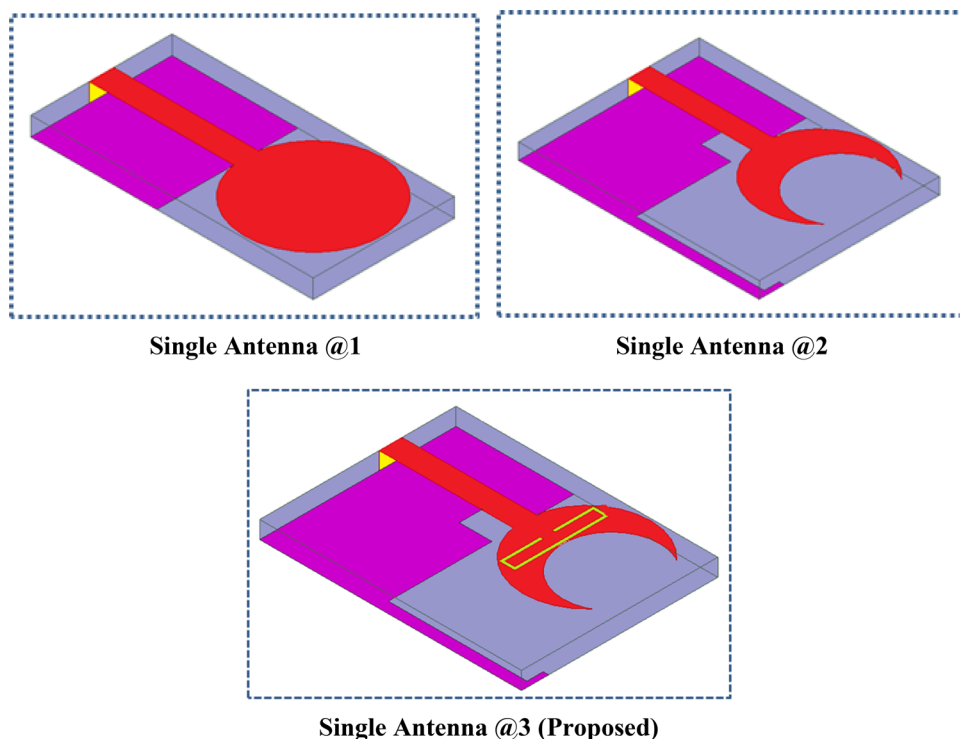


Fig. 4 S_{11} values of evolution steps of proposed single antenna

parameter for analysing mutual coupling effect. The Fig. 10 represents the surface current distributions of proposed single notched MIMO antenna for various frequencies in the working operating region. The Fig. 10(d) shows the SCD representation of proposed work at notched frequency band. From this, it is observed that except slot region remaining part of radiator is not exciting.

2.1.2.4 Time response analysis The time response analysis is required for the estimation of UWB signal transmis-

sion, as a very narrow pulse width in terms of ns are used for the signal transmission. Hence, consideration of input impedance and group delay are required for analysis of UWB signal. The impedance matching between the port and patch of proposed single notched MIMO antenna is well matched, except at the notched band. It maintains 50Ω in real and 0Ω at the imaginary impedances and except at the notched WLAN band, which is clearly given in Fig. 11. At notched band, the real impedance is changed to 300Ω and imaginary impedance is changed to 150Ω . The proposed single notched MIMO antenna maintains 0.25 ns group delay in the entire working band and it is -1.75 ns in the notched band and it is shown in Fig. 12.

2.1.2.5 Characteristic mode analysis (CMA) In the year 1965, Garbacz et al. proposed a new theory named as Characteristic Mode Analysis (CMA). The theory of CMA will help the electrical behaviour of conducting material by observing the surface current distributions on the material [30]. An infinite number of orthogonal currents will flow on the conducting planes and these currents are known as modes. The analysis of modes will give almost better estimation of electrical behaviour of conducting plane and it helps the designing the antenna using full wave simulations like HFSS, CST, FEKO and so on. The number of modes is usually depending on conducting material size. The intrinsic relation between modal currents and modal impedance matrix is shown in Eq. (1) [31].

Fig. 5 Evolution steps of proposed single notched MIMO antenna

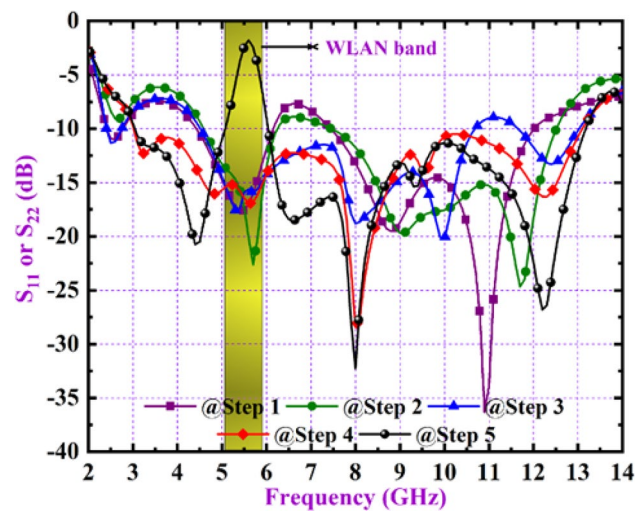
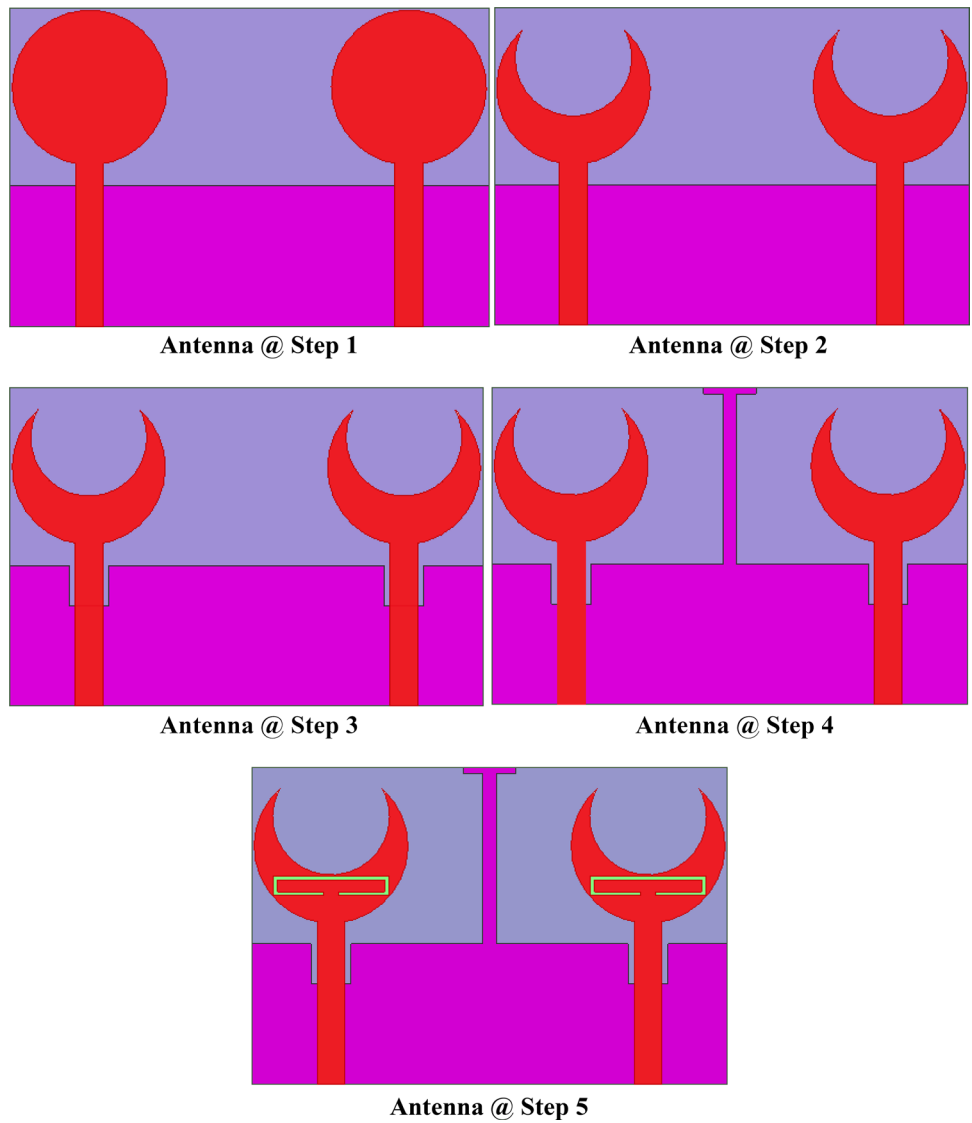


Fig. 6 S_{11} (or) S_{22} values of evolution steps of proposed single notched MIMO antenna

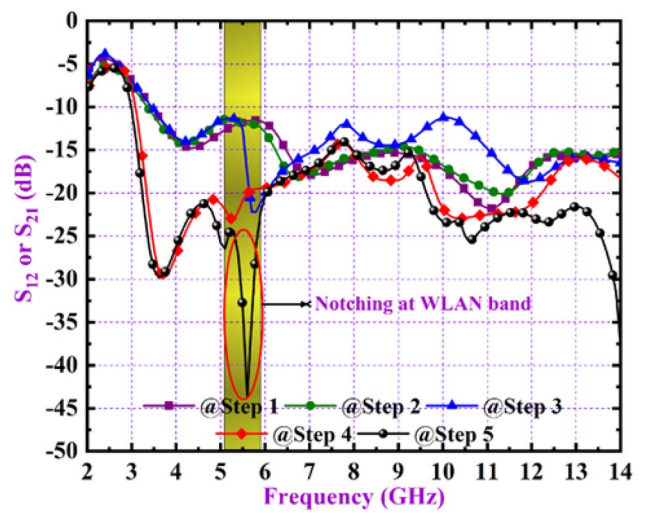
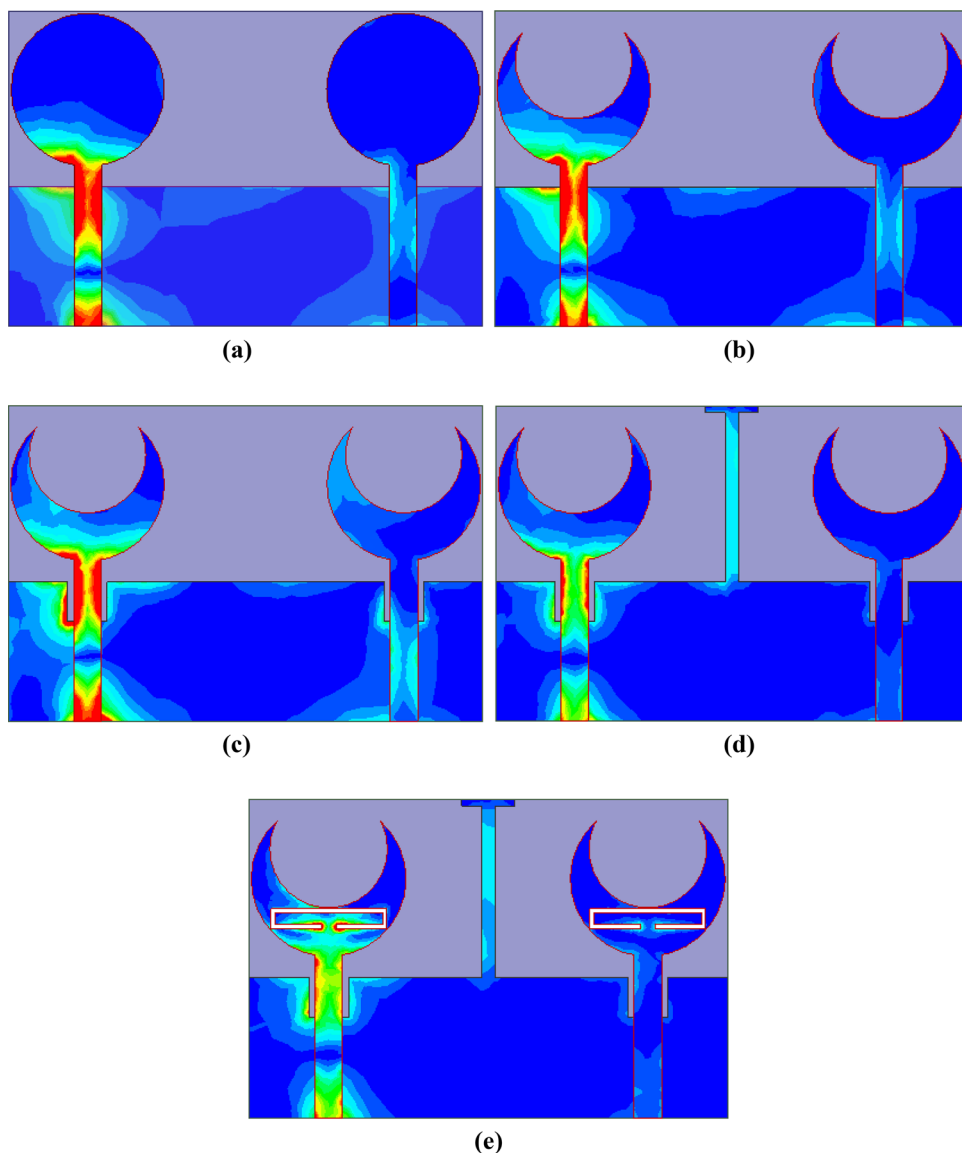


Fig. 7 S_{12} (or) S_{21} values of evolution steps of proposed single notched MIMO antenna

Fig. 8 a–e Surface current distribution of evolution steps of proposed single notched MIMO antenna



$$X(J_n) = \lambda_n R(J_n) \tag{1}$$

where J_n represents the modal currents and λ_n represents the Eigen values. The range of λ_n are $-\infty$ to $+\infty$ and the resonant values are occurred at λ_n is zero. The modal significance (MS) is the parameter is used to identify the resonant frequencies of conducting material and it is related to the Eigen vector. The relation between MS and λ_n is represented in Eq. (2). Another important parameter known as characteristic angle (CA) which is also help the estimation of electrical behaviour of conducting planes. The relation between CA and λ_n is shown in Eq. (3).

$$MS = \left| \frac{1}{1 + j\lambda_n} \right| \tag{2}$$

$$CA = 180^\circ + \tan^{-1}(\lambda_n) \tag{3}$$

The proposed single notched MIMO antenna is checked with theory of characteristic mode analysis in terms of modal significance and characteristic angle. Initially, several modes in the operating bandwidth are identified as given in Fig. 13(a). From these modes, the useful modes contributing to the impedance bandwidth are identified, which are Modes 1, 2, 4, 5, 7, 10, 11, 12, 13, 14 & 15 in the present case. The Fig. 13(a), (c) shows the representation of MS and CA response of the proposed single notched MIMO antenna with 15 modes and some of them are higher order modes. From these figures, it is observed that the S-parameter result of proposed antenna is almost matched with MS and CA responses. The Fig. 13(b), (d) show the characteristic angle representation of modes, including notched mode and also showing the clear observation of notching is occurred

Table 1 Optimisation of parameters with various values

| Parameter | Value (mm) | Impedance bandwidth (GHz) |
|---|-------------------|---------------------------|
| Width of the feed (W_f) | $W_f=1.6$ | 3–8.8 & 11.2–13.1 |
| | $W_f=2.1$ (P*) | 3–13.2 |
| | $W_f=2.6$ | 3.6–13.2 |
| Radius (R_2) | $R_2=3.9$ | 3–3.9 & 4.2–13.5 |
| | $R_2=4.4$ (P*) | 3–13.2 |
| | $R_2=4.9$ | 3–10 & 11–13.1 |
| Length of ground (L_g) | $L_g=10.1$ | 3.1–12.9 |
| | $L_g=10.6$ (P*) | 3–13.2 |
| | $L_g=11.1$ | 3–9.2 & 11–13.1 |
| Width of T-strip at top position (W_3) | $W_3=2$ | 3–13.2 |
| | $W_3=4$ (P*) | 3–13.2 |
| | $W_3=6$ | 3–13.2 |
| Width of T-strip at top position (W_4) | $W_4=1$ (P*) | 3–13.2 |
| | $W_4=2$ | 3.2–10.8 & 11–13.1 |
| | $W_4=3$ | 3–6.8 & 7–13.1 |
| Width of downward direction C-slot (S_{W2}) | $S_{W2}=2.8$ | 3–5.4 & 6.6–13.0 |
| | $S_{W2}=3.3$ | 3–5.3 & 6.4–13.0 |
| | $S_{W2}=3.8$ (P*) | 3–5.1 & 6–13.2 |

WLAN band at mode 8 and these are well matched with S-parameter results of proposed antenna.

2.1.3 Proposed dual notched MIMO antenna evolution

The Fig. 14(a) shows the simulated S-parameters representation of the proposed structure with dual-band notched characteristics. By making slots on radiating patch and feed line, it eliminates the WLAN and complete X-band region. Parametric study has been done on slot length (S_{L3}), which is subtracted from feed line for eliminating complete X-band and are represented in Fig. 14(b), (c). If S_{L3} value is 4 mm, it eliminates the complete X-band region which is from 8 to 12.2 GHz and if it is 4.5 mm it eliminates 7–11.8 GHz band. The band of 6.8–9.2 GHz is rejected when it is 5 mm and 6.5–8.4 GHz band is removed with S_{L3} value taken as 5.5 mm. Table 2 shows the rejected bands with different values of slot length (S_{L3}). From the above information, based on applications, we can choose the S_{L3} value. Here choosing 4 mm as optimised value gives the complete rejection of X-band region. Based on user requirements we can adjust the notching band from 6.5 to 12.2 GHz. The significant novelty of the proposed work is the adjustment of notch bands by controlling S_{L3} parameter as highlighted in Table 2. Earlier works focused on attaining either single notch or dual notch or triple notch, whereas the current work presents the design of a novel antenna with adjustable notch bands.

The surface current distributions of the proposed design at dual-notched bands 5.5 GHz and 11.4 GHz when port 1 is excited are represented in Fig. 15. From the obtained surface current distribution, it is observed that the antenna

element does not radiate at notched region and only slot positions are radiating, and are clearly shown in Fig. 15(a), (b).

The negative peak gain values are achieved at the notched bands and is mentioned in Fig. 16(a). The same results are verified with 3D polar radiation patterns at notched bands. The radiation characteristics (3D-Polar plot) of proposed design at dual-notched bands are represented in Fig. 16(b), (c). From the Fig. 5 it is clear that negative gain values are occurred at notch bands. At 5.6 GHz a negative gain of -2.62 dBi and at 10.3 GHz a negative gain of -1.44 dBi are achieved.

The notched bands in the UWB region of proposed dual-notched MIMO antenna are obtained by making slots on the radiating patch and feed line. The width of the slot will affect the notched characteristics slightly, but the length of the slot has more impact on the notched resonant band. The overall length of slot should be one half or quarter wave length of centre frequency of notched band. Here, λ represents the guided wavelength and it is represented using Eq. (4). The half & quarter wave length for notched band characteristics equations are represented using Eqs. (5) and (6) [27, 28]. The $\lambda/2$ wave equation for the proposed dual notched MIMO antenna are presented using Eqs. (7) and (8)

$$\lambda = \frac{C}{f_{notch} \sqrt{\epsilon_{eff}}}; \quad \epsilon_{eff} = \frac{1 + \epsilon_r}{2} \quad (4)$$

ϵ_{eff} is effective dielectric constant.

For $\lambda/2$ wave representation

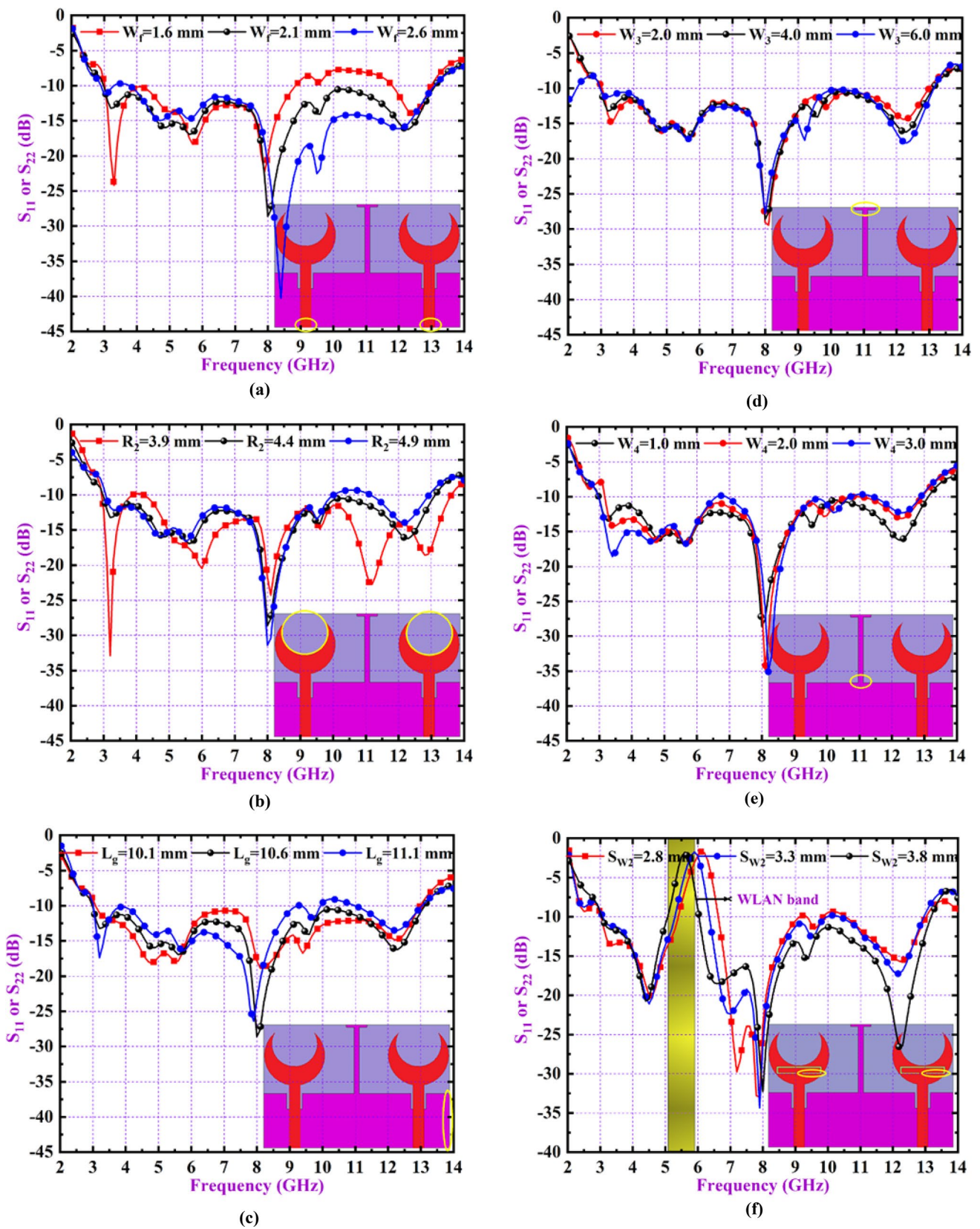


Fig. 9 Parameters optimisations of proposed MIMO antenna; a W_1 ; b R_2 ; c L_g ; d W_3 ; e W_4 and f S_{W_2}

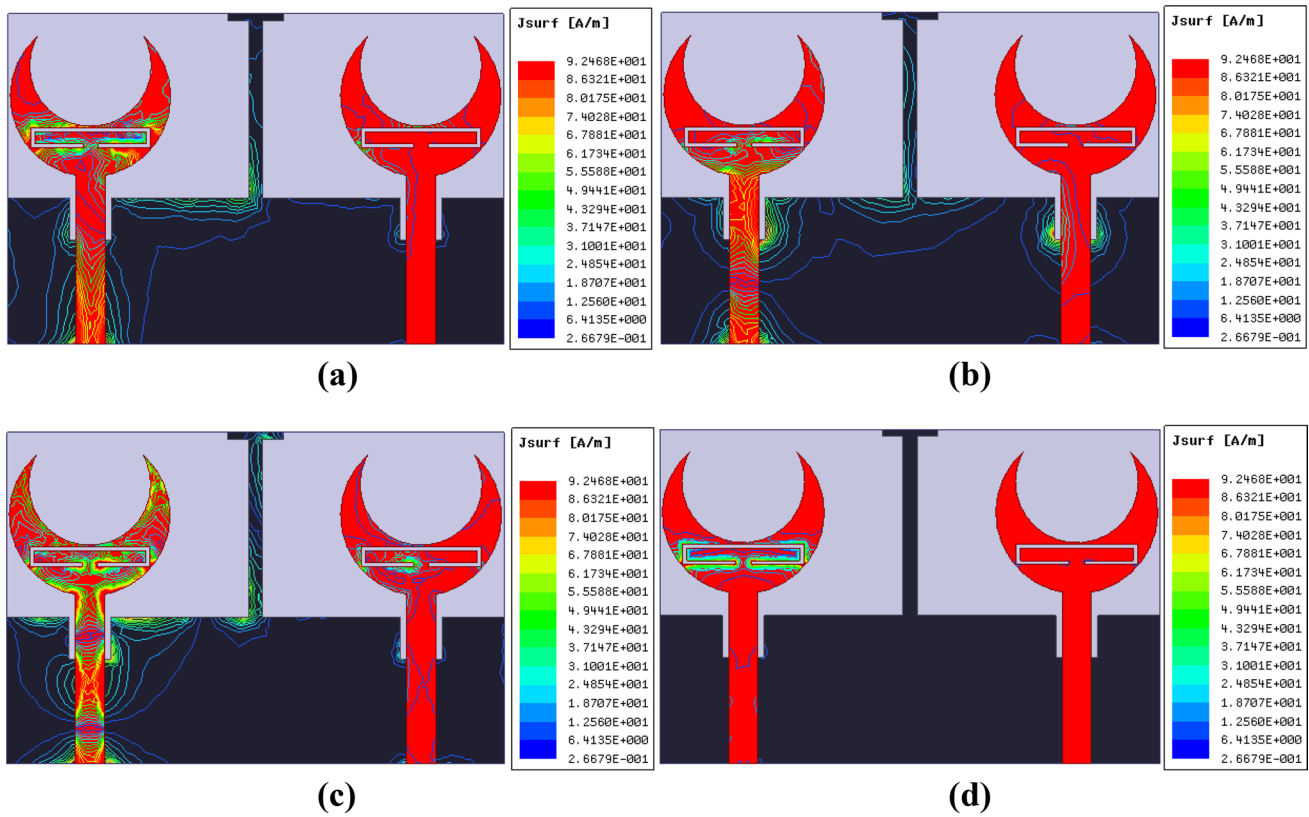


Fig. 10 Surface current distribution of proposed single notched MIMO antenna; a 4.4 GHz; b 8.0 GHz; c 12.2 GHz and d 5.6 GHz (notched band)

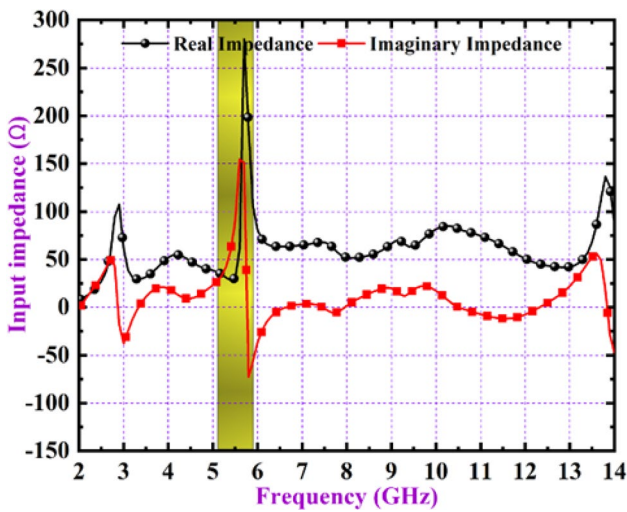


Fig. 11 Input impedance response of proposed single notched MIMO antenna

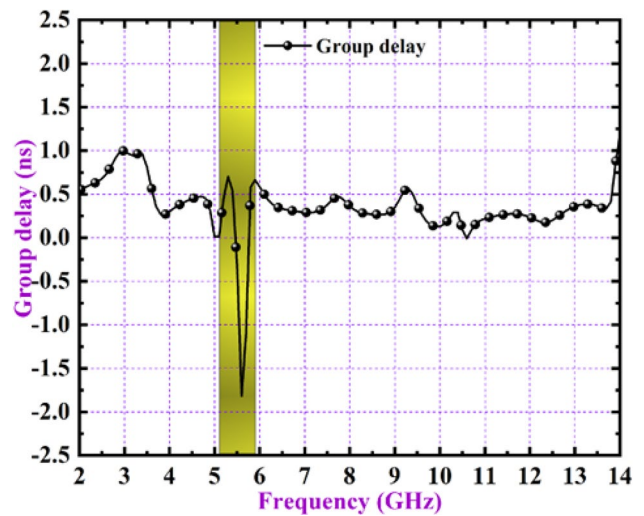


Fig. 12 Group delay response of proposed single notched MIMO antenna

$$L_{notch} = \frac{C}{2f_{notch}\sqrt{\epsilon_{eff}}} = \frac{\lambda}{2} \tag{5}$$

For $\lambda/4$ wave representation

$$L_{notch} = \frac{C}{4f_{notch}\sqrt{\epsilon_{eff}}} = \frac{\lambda}{4} \tag{6}$$

From the proposed dual notched MIMO antenna

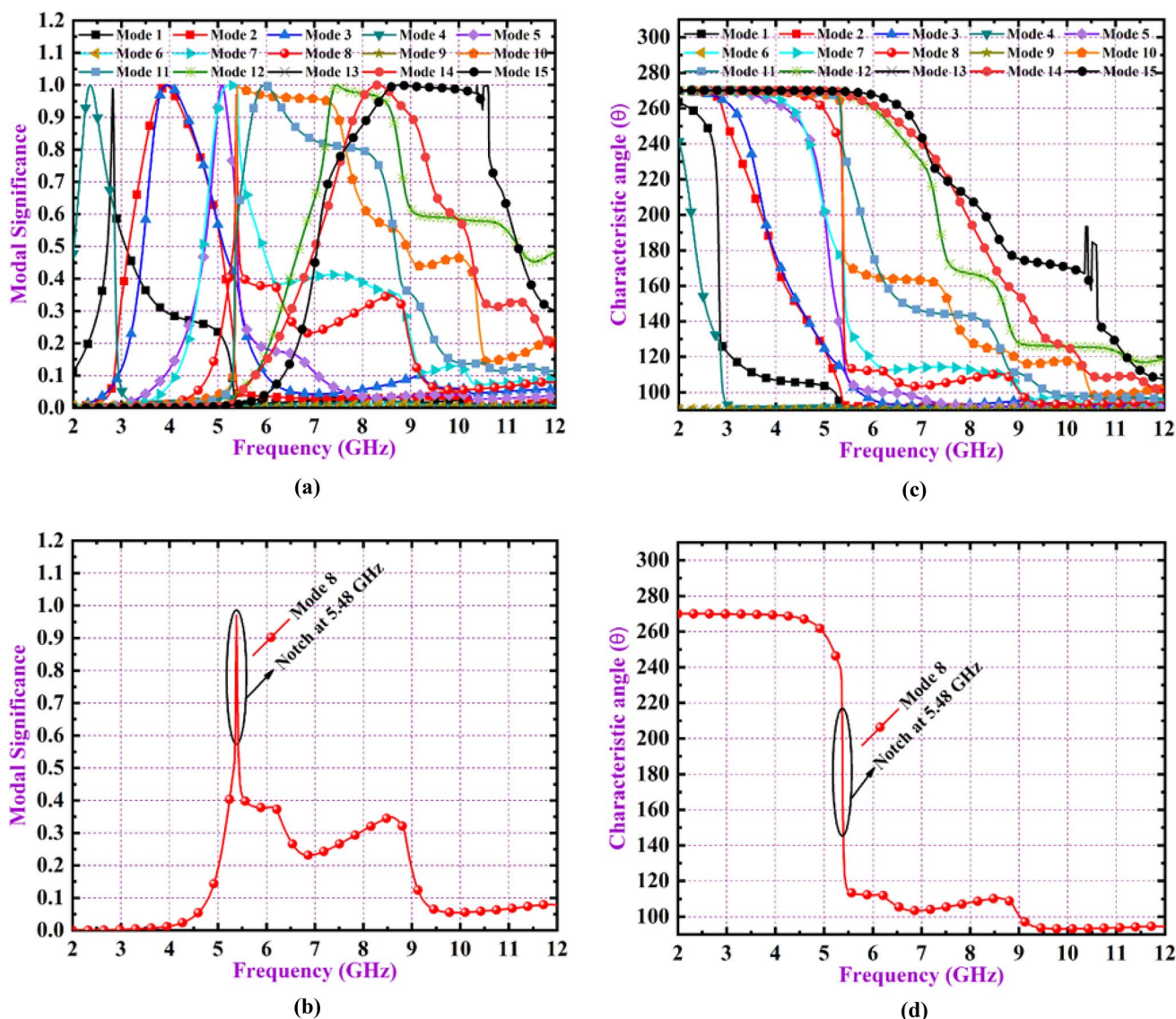


Fig. 13 Proposed single notched MIMO antenna CMA results; **a** modal significance with 15 modes; **b** modal significance at notched band; **c** characteristic angle with 15 modes and **d** characteristic angle at notched band

$$L_{notch}(at\ 5.6\ GHz) = 2(S_{L2} + S_{W2}) + S_{W1} - 2(S_{L1}) \approx \frac{\lambda}{2} \tag{7}$$

$$L_{notch}(at\ 10.3\ GHz) = S_{L3} + S_{W3} + S_{L4} - 2(S_{W4}) \approx \frac{\lambda}{2} \tag{8}$$

The parameters TARC and CCL are very much useful for analysing the diversity characteristics of MIMO antenna. TARC gives the overall system reflection coefficient results by considering the changes in self and mutual impedances and the CCL describes the number transmitted bits losses due to coupling at transmitting end while transmission [29]. The proposed structure TARC and CCL responses are represented in Fig. 6. The acceptable TARC and CCL values

when transmitting signals are ≤ 0 dB and ≤ 0.4 bits/s/Hz respectively. The proposed structure giving good TARC and CCL values which are below -10 dB and ≤ 0.1 bits.s/Hz. From the Fig. 17, it is clearly observed that perfect notching is occurred at desired bands and in TARC responses also.

3 Experimental verification of simulation results

3.1 S-Parameters

The first and fore most parameter deciding the radiation of the patch is the reflection coefficient. Similarly,

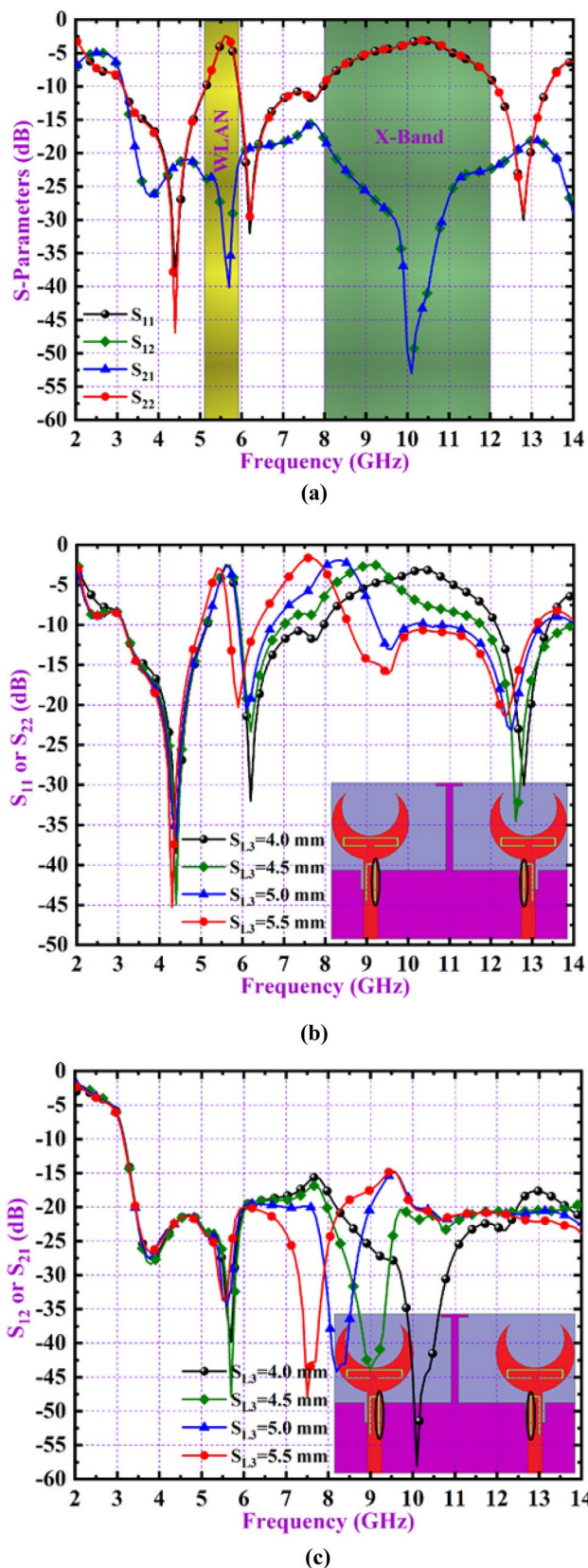


Fig. 14 **a** Simulated S-parameters of proposed dual notched MIMO antenna **a** dual notched characteristics; **b** parametric analysis of S_{L3} for S_{11} results and **c** parametric analysis of S_{L3} for S_{21} results

transmission coefficient is another parameter defining the radiation effect of one radiator on the other. The proposed single notched MIMO antenna is fabricated and tested. The measured results are almost well matched with simulated one. The simulated S_{11} results are obtained in the band 3–13.2 GHz working band and measured results are obtained in the band 3.1–13 GHz. The Fig. 18(a) show the S-parameters response of proposed single notched design. The top and bottom views of the fabricated proposed single notched MIMO antenna are shown in Fig. 18(c), (d).

3.2 Diversity metric characteristics

The essential parameters for characterising the MIMO antenna system are ECC, DG, TARC, CCL and MEG. The metric ECC describes the correlation between the channels in the MIMO system. It is calculated in different ways like using S-parameters, far-field patterns and S-parameters with radiation efficiency values. Of all these, using S-parameters is simple and easy to calculate the ECC value. The acceptable value of ECC is below 0.5 in practical applications. The proposed design gives ECC values less than 0.01 and here the ECC values are calculated using S-parameters. The ideal value of DG is 10 dB and the proposed design gives the DG values above 9.98 dB. The ECC in terms of S-parameters and DG in terms of ECC are represented in Eqs. (3) and (4) [32, 33]. The Fig. 19(a), (b) depict the ECC and DG values of the proposed design's simulated and measured results.

$$ECC = \frac{|S_{11}^* S_{12} + S_{12}^* S_{22}|^2}{(1 - |S_{11}|^2 - |S_{21}|^2)(1 - |S_{22}|^2 - |S_{12}|^2)} \quad (9)$$

$$DG = 10\sqrt{1 - ECC^2} \quad (10)$$

The active reflection coefficient is not sufficient for analysing the overall system MIMO performance. While, transmitting the signals from the MIMO system simultaneously, there is chance of altering the self and mutual impedances of the radiators due to radiation effects of one antenna on the other. Hence, a new metric is defined named as TARC. It considers the changes in the self and mutual impedance of all the radiators in the MIMO system. The proposed design gives perfect TARC values with exclusion of notched band and these are clearly shown in Fig. 19(c). In the working band of proposed design, the TARC values are below -10 dB and the equation is represented in (5) using S-parameters [34].

Table 2 Slot length (S_{L3}) variations with corresponding rejection bands

| Slot length (S_{L3}) | Rejection band | Applications of rejected band |
|--------------------------|----------------|--|
| 4.0 mm (P*) | 8.0–12.2 GHz | Complete X-band only |
| 4.5 mm | 7–11.8 GHz | Satellite up & down link and complete X-band |
| 5.0 mm | 6.8–9.2 GHz | INSAT-C band and Satellite up & down link |
| 5.5 mm | 6.5–8.4 GHz | INSAT-C band and Satellite up & down link only |

Fig. 15 Surface current distribution at notched bands; **a** 5.6 GHz and **b** 10.3 GHz

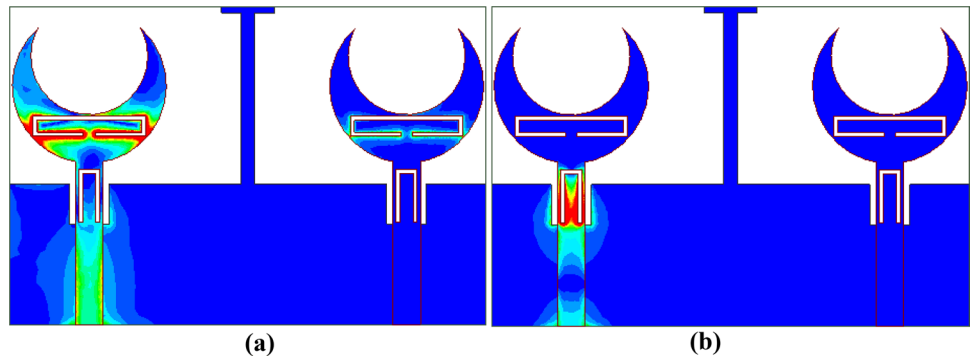
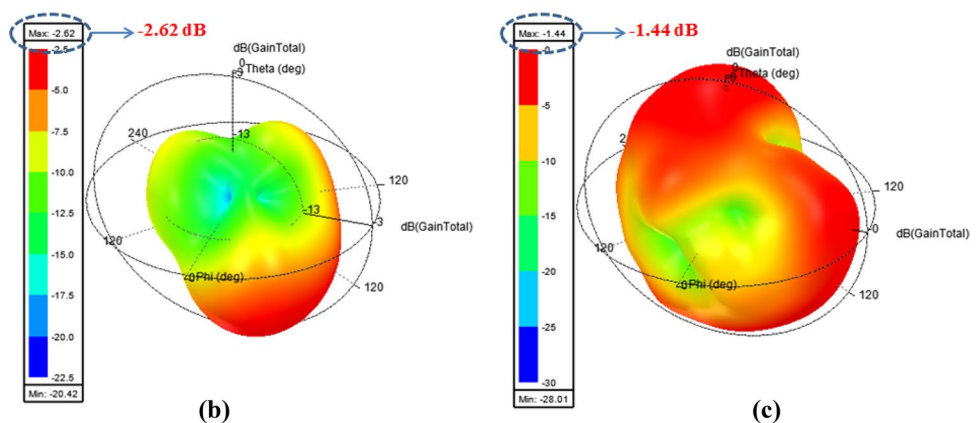
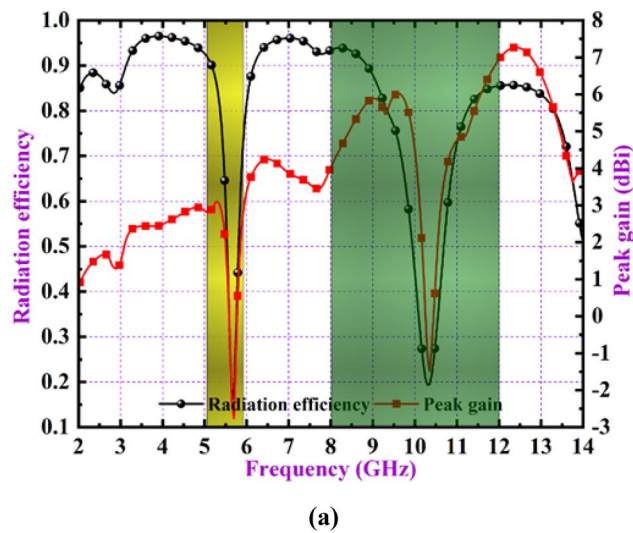


Fig. 16 3D radiation patterns at notched bands; **a** The negative peak gain values are achieved at the notched band frequencies of 5.6 GHz and 10.3 GHz are -2.62 dBi and -1.44 dBi, respectively **b** 5.6 GHz and **c** 10.3 GHz



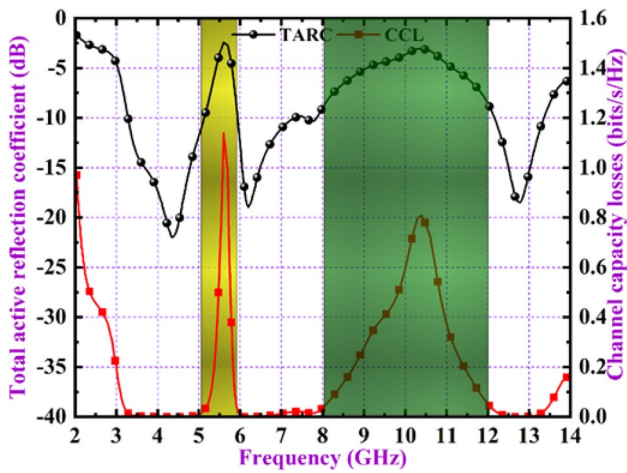


Fig. 17 Simulated TARC and CCL values of proposed dual notched design

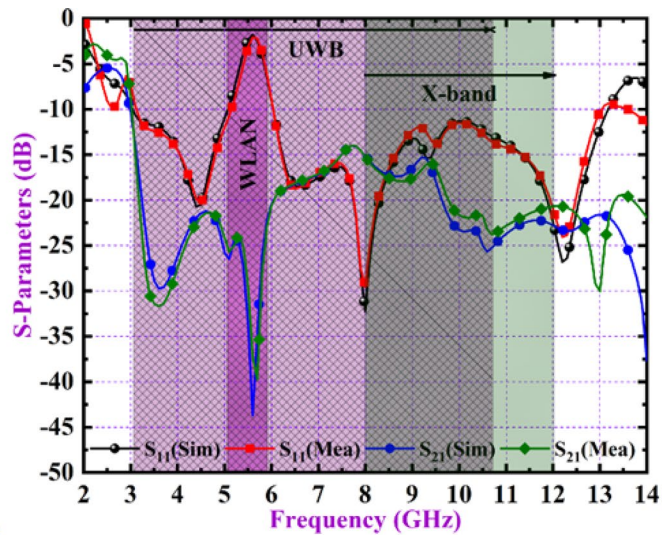
$$TARC = \sqrt{\frac{|(S_{11} + S_{12}e^{j\theta})|^2 + |(S_{21} + S_{22}e^{j\theta})|^2}{2}} \quad (11)$$

And, while transmitting the signals, there is chance to losses the bits due to collision between the radiation patterns. The metric CCL describes the number of bits lost, while signal is transmitted. Here the CCL parameter is calculated using S-parameters and these values are below 0.1 bits/s/Hz and are achieved except at the notched band as shown in Fig. 19(d). The CCL is represented in Eq. (6), the acceptable values of CCL are below 0.4 bits/s/Hz in practical applications.

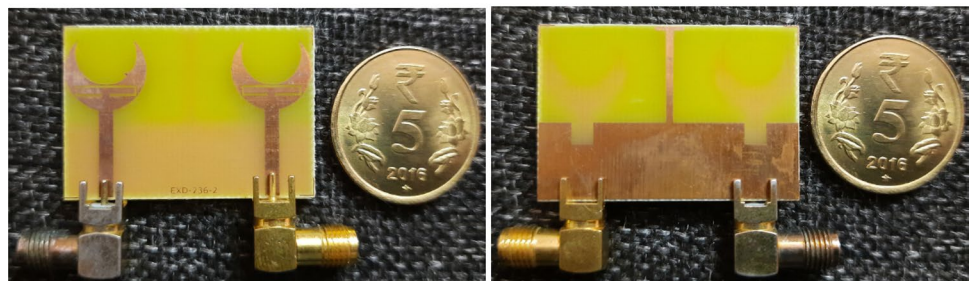
$$C_{Loss} = -\log_2 \det(\alpha^R) \quad (12)$$

where,

Fig. 18 Simulation and measured results of proposed single notched MIMO antenna; **a** S-parameters; **b** top layer and **c** bottom layer



(a)



(c)

(d)

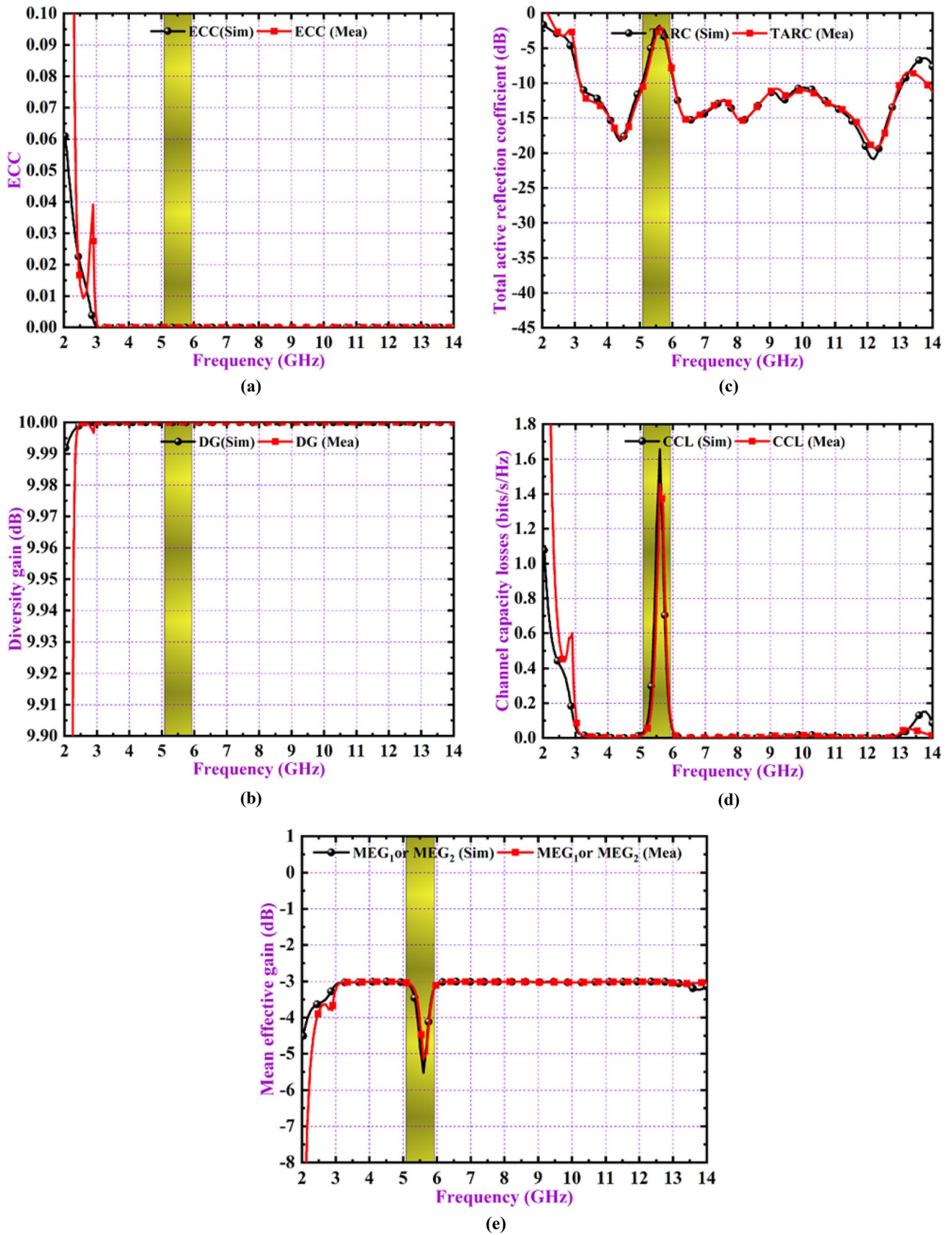


Fig. 19 Simulation and measured results of proposed single notched MIMO antenna; a ECC; b DG; c TARC; d CCL and e MEG

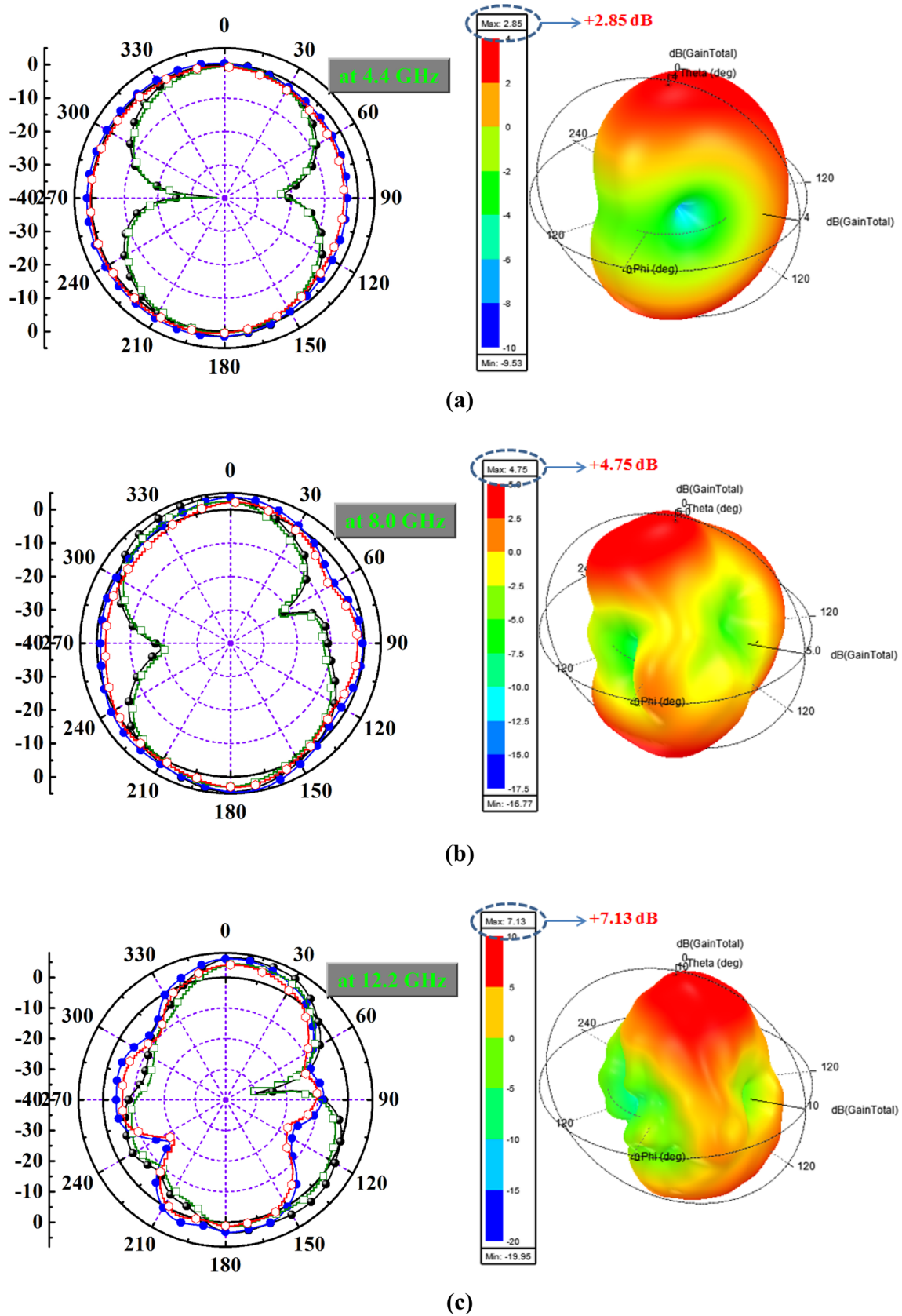


Fig. 20 Simulation & measured (E & H) Fields and 3D polar plot representation of proposed single notched MIMO antenna; **a** 4.4 GHz; **b** 8.0 GHz; **c** 12.2 GHz and **d** 5.6 GHz (notched band)

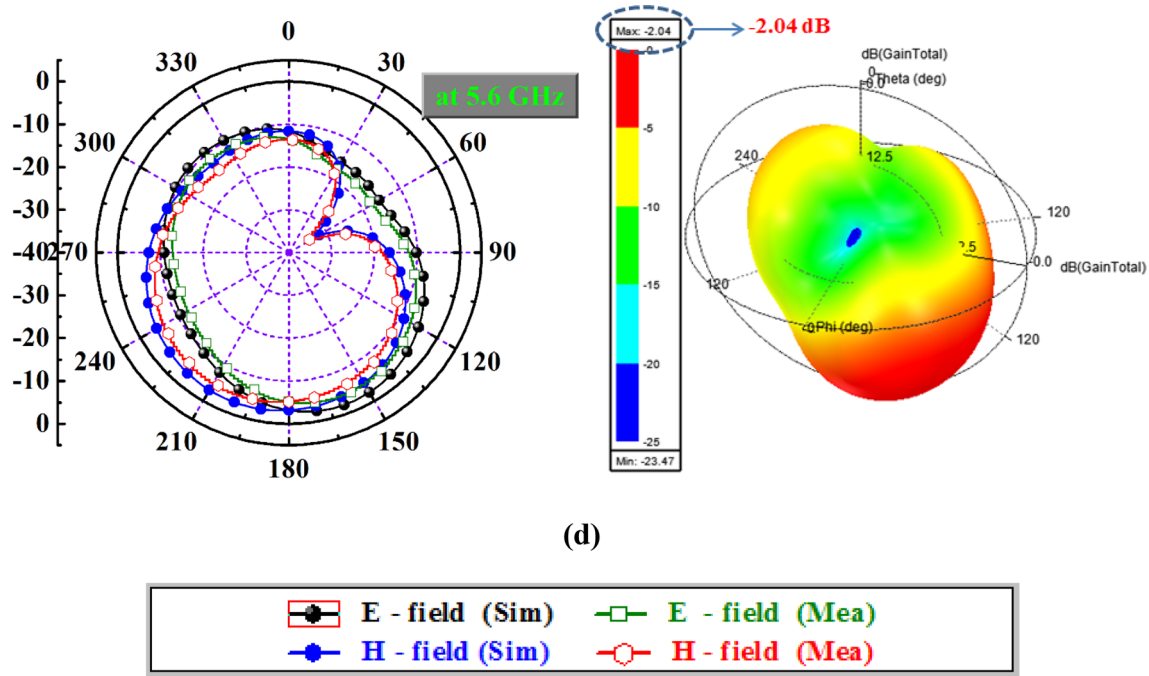


Fig. 20 (continued)

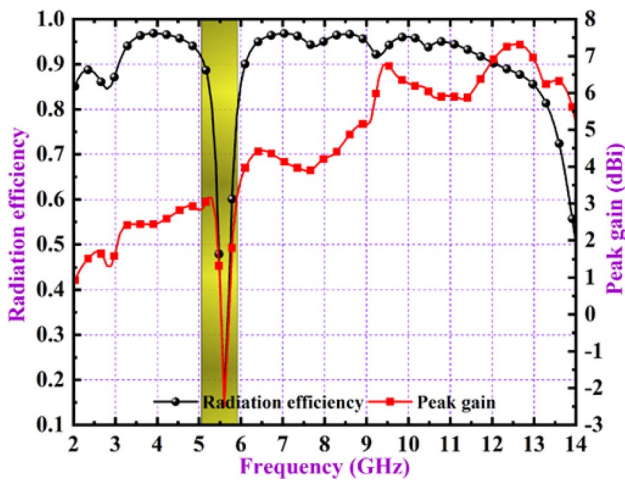


Fig. 21 Simulated radiation efficiency and peak gain values of proposed single notched MIMO antenna

$$\alpha^R = \begin{bmatrix} \alpha_{ii} & \alpha_{ij} \\ \alpha_{ji} & \alpha_{jj} \end{bmatrix}$$

$$\alpha_{ii} = 1 - \left(|S_{ii}|^2 + |S_{ij}|^2 \right); \quad \alpha_{ij} = - \left(S_{ii}^* S_{ij} + S_{ji}^* S_{jj} \right);$$

$$\alpha_{ji} = - \left(S_{jj}^* S_{ji} + S_{ij}^* S_{ii} \right); \quad \alpha_{jj} = 1 - \left(|S_{jj}|^2 + |S_{ji}|^2 \right).$$

The receiving ability of the receiver is decided by the factor MEG. In MIMO system, the signals are transmitted and received in different paths and MEG is the factor describing the ability of the receiver to receive the signal. The ideal value of MEG is -3 dB and the proposed design is giving MEG values approximately -3 dB [35, 36]. At the notched band, it is clearly observed that the MEG values are around -6 dB and it is clearly shown in Fig. 19(e). The equation of MEG in terms of S-parameters is represented in (7).

$$MEG_i = 0.5\eta_{i,rad} = 0.5 \left[1 - \sum_{j=1}^M |S_{ij}|^2 \right] \tag{13}$$

3.3 Radiation characteristics

The radiation characteristics of the proposed single notched MIMO antenna in terms of 2D and 3D electric and magnetic fields are depicted in Fig. 20. The proposed design gives stable radiation patterns as well as bore sight direction patterns in the UWB region. The peak gain values of the design at various resonant frequencies in 3D polar plots are presented and from these it is clear that positive and high gain values are achieved in the working region. At 4.4 GHz, 8 GHz and 12.2 GHz frequencies, the obtained gain values are 2.85 dBi, 4.75 dBi and 7.13 dBi respectively in 3D polar plots. At 5.6 GHz, a negative peak gain value of -2.04 dB is obtained and it is clearly shown Fig. 20(d).

Table 3 Comparison of proposed work with other literature works

| Ref. no. | Overall size (λ_0) | IBW (GHz) | Isolation (dB) | Notched bands | Max. P.G (dBi) | Max. R.E (%) | TARC (dB) | CCL (bits/s/Hz) |
|----------|------------------------------|-----------|----------------|--------------------|----------------|--------------|-----------|-----------------|
| [5] | 0.35×0.50 | 3–11 | 25 | – | 6 | 95 | – | – |
| [8] | 0.34×0.47 | 3.1–10.6 | 20 | – | 5.3 | 85 | – | – |
| [9] | 0.26×0.40 | 3.1–10.6 | 15 | – | 6.5 | 80 | – | – |
| [10] | 0.26×0.26 | 3.1–10.6 | 15 | – | 4.2 | – | – | – |
| [11] | 0.35×0.35 | 3–12 | 20 | 5.15–5.92 | – | – | – | – |
| [12] | 0.58×0.35 | 3.4–15 | 16 | 3.96–6.2 | 5 | 80 | – | ≤0.4 |
| [13] | 0.15×0.26 | 2–12 | 20 | 4.8–6.2 | – | – | – | – |
| [14] | 0.60×0.36 | 2.2–13.3 | 15 | 4.4–6.2 | 4.7 | 80 | – | – |
| [15] | 0.34×0.50 | 3.1–10.6 | 20 | 5.2–5.6 | 1.6 | – | – | – |
| [16] | 0.39×0.39 | 3.08–11.8 | 15 | 5.03–5.97 | 3.6 | 75 | – | – |
| [17] | 0.40×0.40 | 2.5–12 | 15 | 5.1–6 | 3 | – | – | – |
| [18] | 0.45×0.45 | 2.7–10.7 | 15 | 4.75–12 | 5.2 | 82 | – | – |
| [19] | 0.88×0.56 | 3.1–10.6 | 17.2 | 5.15–5.85 | 5.1 | 95 | – | – |
| [20] | 0.32×0.32 | 3.2–10.4 | 15 | 5.15–5.85, 7.9–8.4 | – | – | – | – |
| [21] | 0.45×0.45 | 3.4–12 | 15 | 5.2–5.8, 7.6–7.9 | 5.5 | – | – | – |
| [22] | 0.17×0.32 | 2.9–20 | 22 | 5.1–5.8, 6.7–7.1 | 7 | 85 | –20 | – |
| [23] | 0.26×0.15 | 3.1–35 | 24 | 5.1–5.8, 6.7–7.1 | 5 | 55 | –20 | – |
| [25] | 0.42×0.21 | 3.1–10.8 | 15 | 5.15–5.85, 7.9–8.4 | 3 | – | – | – |
| P* | 0.24×0.37 | 3.1–13.4 | 22 | 5.15–5.85, 8–12 | 7.4 | 97 | –10 | ≤0.1 |

IBW impedance bandwidth, P.G peak gain, R.E radiation efficiency, P* proposed work

The peak gain and radiation efficiency results of the proposed single notched MIMO antenna is represented in Fig. 21. From the Fig. 21, it is clearly shown that at notched band, the negative peak gain values and low efficiency values are attained. The peak gain values change from 2.3 to 7.4 dBi and efficiency values change from 86 to 97% in the working region. The comparison of proposed work with other listed works are represented in Table 3.

4 Conclusions

A compact MIMO antenna is designed for UWB band applications with rejection of WLAN and complete X-band region is presented in this work. The proposed design is working in the region of 3.1–13.4 GHz and an isolation more than 22 dB is obtained in the majority of the band. The diversity metrics ECC, DG, TARC, CCL and MEG are studied, analysed and attained acceptable values. The radiation characteristics in terms of radiation patterns, efficiency and peak gain parameters are studied and presented. The negative peak values of the design in the notched band are clearly represented in 3D polar plot representation also. The maximum peak gain of 7.14 dBi and maximum efficiency of 97% are attained. The measured results of the design are well

agreed the simulated results and checked with characteristic mode analysis.

Data availability The authors confirm that the data supporting the findings of this study are available within the article. Raw data that support the finding of this study are available from the corresponding author, upon reasonable request.

References

- Coase, R. H. (1959). The federal communications commission. *The Journal of Law and Economics*, 2, 1–40.
- Addepalli, T., & Anitha, V. R. (2022). Parametric analysis of compact UWB-MIMO antenna with improved isolation using parasitic reflectors and protruded ground strips. *Wireless Personal Communications*, 123, 2209–2225.
- Nadeem, I., & Choi, D.-Y. (2018). Study on mutual coupling reduction technique for MIMO antennas. *IEEE Access*, 7, 563–586.
- Addepalli, T., & Anitha, V. R. (2021). Design and analysis of a novel compact spanner-shaped ultra-wideband antenna for MIMO systems. *International Journal of Communication Systems*, 34(5), e4739.
- Wang, L., Du, Z., Yang, H., Ma, R., Zhao, Y., Cui, X., & Xi, X. (2019). Compact UWB MIMO antenna with high isolation using fence-type decoupling structure. *IEEE Antennas and Wireless Propagation Letters*, 18(8), 1641–1645.

6. Jiang, T., Jiao, T., & Li, Y. (2018). A low mutual coupling MIMO antenna using periodic multi-layered electromagnetic band gap structures. *Applied Computational Electromagnetics Society Journal*, 33(3), 305.
7. Yu, K., Li, Y., & Liu, X. (2018). Mutual coupling reduction of a MIMO antenna array using 3-D novel meta-material structures. *Applied Computational Electromagnetics Society Journal*, 33(7), 758–763.
8. Khan, M. S., Capobianco, A. D., Najam, A. I., Shoaib, I., Autizi, E., & Shafique, M. F. (2014). Compact ultra-wideband diversity antenna with a floating parasitic digitated decoupling structure. *IET Microwaves, Antennas & Propagation*, 8(10), 747–753.
9. Liu, L., Cheung, S. W., & Yuk, T. I. (2013). Compact MIMO antenna for portable devices in UWB applications. *IEEE Transactions on antennas and propagation*, 61(8), 4257–4264.
10. Zhang, J. Y., Zhang, F., Tian, W. P., & Luo, Y. L. (2015). ACS-fed UWB-MIMO antenna with shared radiator. *Electronics Letters*, 51(17), 1301–1302.
11. Zhu, J., Li, S., Feng, B., Deng, L., & Yin, S. (2015). Compact dual-polarized UWB quasi-self-complementary MIMO/diversity antenna with band-rejection capability. *IEEE Antennas and Wireless Propagation Letters*, 15, 905–908.
12. Kumar, A., Ansari, A. Q., Kanaujia, B., Kishor, J., & Tewari, N. (2018). Design of triple-band MIMO antenna with one band-notched characteristic. *Progress In Electromagnetics Research C*, 86, 41–53.
13. Khan, M. S., Capobianco, A. D., Naqvi, A., Shafique, M. F., Ijaz, B., & Braaten, B. D. (2015). Compact planar UWB MIMO antenna with on-demand WLAN rejection. *Electronics Letters*, 51(13), 963–964.
14. Toktas, A. (2017). G-shaped band-notched ultra-wideband MIMO antenna system for mobile terminals. *IET Microwaves, Antennas & Propagation*, 11(5), 718–725.
15. Yoon, H. K., Yoon, Y. J., Kim, H., & Lee, C. H. (2011). Flexible ultra-wideband polarisation diversity antenna with band-notch function. *IET Microwaves, Antennas & Propagation*, 5(12), 1463–1470.
16. Kang, L., Li, H., Wang, X., & Shi, X. (2015). Compact offset microstrip-fed MIMO antenna for band-notched UWB applications. *IEEE Antennas and Wireless Propagation Letters*, 14, 1754–1757.
17. Gao, P., He, S., Wei, X., Xu, Z., Wang, N., & Zheng, Y. (2014). Compact printed UWB diversity slot antenna with 5.5-GHz band-notched characteristics. *IEEE Antennas and Wireless Propagation Letters*, 13, 376–379.
18. Chacko, B. P., Augustin, G., & Denidni, T. A. (2013). Uniplanar polarisation diversity antenna for ultra-wideband systems. *IET Microwaves, Antennas & Propagation*, 7(10), 851–857.
19. Lee, J. M., Kim, K. B., Ryu, H. K., & Woo, J. M. (2012). A compact ultra-wideband MIMO antenna with WLAN band-rejected operation for mobile devices. *IEEE Antennas and Wireless Propagation Letters*, 11, 990–993.
20. Zhu, J., Feng, B., Peng, B., Deng, L., & Li, S. (2016). A dual notched band MIMO slot antenna system with Y-shaped defected ground structure for UWB applications. *Microwave and Optical Technology Letters*, 58(3), 626–630.
21. Zhu, J., Feng, B., Peng, B., Li, S., & Deng, L. (2016). Compact CPW UWB diversity slot antenna with dual band-notched characteristics. *Microwave and Optical Technology Letters*, 58(4), 989–994.
22. Chandel, R., Gautam, A. K., & Rambabu, K. (2018). Tapered fed compact UWB MIMO-diversity antenna with dual band-notched characteristics. *IEEE Transactions on Antennas and Propagation*, 66(4), 1677–1684.
23. Gautam, A. K., Yadav, S., & Rambabu, K. (2018). Design of ultra-compact UWB antenna with band-notched characteristics for MIMO applications. *IET Microwaves, Antennas & Propagation*, 12(12), 1895–1900.
24. Sharma, M., Awasthi, Y. K., & Singh, H. (2017). Planar high rejection dual band-notch UWB antenna with X & Ku-bands wireless applications. *International Journal of Microwave and Wireless Technologies*, 9(8), 1725–1733.
25. Salamin, M. A., Das, S., & Zugari, A. (2020). Closed loop resonator based compact UWB antenna with single notched band varying between WLAN and X-band for UWB applications. *Frequenz*, 74(5–6), 201–209.
26. Wang, X., & Sun, Y. (2020). Ultra-wideband MIMO antenna with double notched band. In *2020 cross strait radio science & wireless technology conference (CSRSWTC)*. IEEE.
27. Kumar, A., Ansari, A. Q., Kanaujia, B. K., Kishor, J., & Kumar, S. (2020). An ultra-compact two-port UWB-MIMO antenna with dual band-notched characteristics. *AEU-International Journal of Electronics and Communications*, 114, 152997.
28. Zheng, Z. A., Chu, Q. X., & Tu, Z. H. (2010). Compact band-rejected ultra-wideband slot antennas inserting with $\lambda/2$ and $\lambda/4$ resonators. *IEEE Transactions on Antennas and Propagation*, 59(2), 390–397.
29. Addepalli, T., & Anitha, V. R. (2020). Compact two-port MIMO antenna with high isolation using parasitic reflectors for UWB, X and Ku band applications. *Progress In Electromagnetics Research C*, 102, 63–77.
30. Garbacz, R. J. (1965). Modal expansions for resonance scattering phenomena. *Proceedings of the IEEE*, 53(8), 856–864.
31. Mohanty, A., & Behera, B. R. (2021). Characteristics mode analysis: a review of its concepts, recent trends, state-of-the-art developments and its interpretation with a fractal UWB MIMO antenna. *Progress in Electromagnetics Research B*, 92, 19–45.
32. Sharawi, M. S., Hassan, A. T., & Khan, M. U. (2017). Correlation coefficient calculations for MIMO antenna systems: A comparative study. *International Journal of Microwave and Wireless Technologies*, 9(10), 1991–2004.
33. Addepalli, T., & Anitha, V. R. (2020). A very compact and closely spaced circular shaped UWB MIMO antenna with improved isolation. *AEU-International Journal of Electronics and Communications*, 114, 153016.
34. Fritz-Andrade, E., Jardon-Aguilar, H., & Tirado-Mendez, J. A. (2020). The correct application of total active reflection coefficient to evaluate MIMO antenna systems and its generalization to N ports. *International Journal of RF and Microwave Computer-Aided Engineering*, 30(4), e22113.
35. Glazunov, A. A., Molisch, A. F., & Tufvesson, F. (2009). Mean effective gain of antennas in a wireless channel. *IET Microwaves, Antennas & Propagation*, 3(2), 214–227.
36. Balaji, V. R., Addepalli, T., Desai, A., Nella, A., & Nguyen, T. K. (2021). An inverted L-strip loaded ground with hollow semi-hexagonal four-element polarization diversity UWB-MIMO antenna. *Transactions on Emerging Telecommunications Technologies*, 33, e4381.

Publisher's Note Springer Nature remains neutral with regard to jurisdictional claims in published maps and institutional affiliations.

Springer Nature or its licensor (e.g. a society or other partner) holds exclusive rights to this article under a publishing agreement with the author(s) or other rightsholder(s); author self-archiving of the accepted manuscript version of this article is solely governed by the terms of such publishing agreement and applicable law.



B. Rama Rao working as Professor & HOD of ECE Department, Aditya Institute of Technology and Management, Tekkali. He completed his B.E., Master of Technology in the stream of Radar and microwave engineering from Andhra University. He awarded Ph.D in June 2015 in Electronics and Communication Engineering specialized with “Design of Microstrip patch antenna for wireless Communication Applications” from Andhra University, Visakhapatnam. He has been working in

this college since 2008 and having 23 years of experience in teaching & research. He has published 28 papers in reputed International journal with good impact factor and Scopus indexed, attended 12 National and International conferences. He acted as a reviewer of International journals and chaired conferences. Three research scholars are pursuing Ph.D under his guidance. He is the senior member of IEEE, Life member of IETE and ISTE. His area of interests are Antenna and wave propagation, Microwave and Radar systems etc.



K. S. Chakradhar working as Associate Professor in Department of ECE, Sree Vidyanikethan Engineering College, Tirupathi. He completed his B.Tech from JNTU Kakinada, Master of Engineering from Satyabhama Deemed University, Chennai. He awarded Ph.D in January 2022 in Electronics and Communication Engineering from GITAM deemed to be university, Visakhapatnam. He has 21 years of experience in teaching & research. He has published 15 papers in reputed National and

International journal with good impact factor and Scopus indexed, attended 05 National and International conferences.. He is Life member

of ISTE and Indian Science Congress His area of interests are Microstrip Patch Antennas and image processing.



D. Nataraj working as Professor in Department of ECE, Pragati Engineering College, Kakinada. He received B.Tech. in Electronics and Communication from JNTU, Kakinada, M.Tech in Electronics and Communication Engineering from JNTU, Hyderabad and Ph.D. in Wireless Communication from GITAM, Deemed to be university, Visakhapatnam, Andhra Pradesh. He has more than 20 years of teaching and research experience. His research interests are design of antennas for

various applications, MIMO antennas, wearable, optically transparent antenna and dielectric resonator antenna, design of reflector antenna. He had published around 20 papers in national and international journal/conference and has published 6 Patents.